



**HAL**  
open science

## Reactivity enhancement of gasification biochars for catalytic applications

Marion Ducouso, Elsa Weiss-Hortala, Ange Nzihou, Marco J. Castaldi

► **To cite this version:**

Marion Ducouso, Elsa Weiss-Hortala, Ange Nzihou, Marco J. Castaldi. Reactivity enhancement of gasification biochars for catalytic applications. *Fuel*, 2015, 159, p. 491-499. 10.1016/j.fuel.2015.06.100 . hal-01609221

**HAL Id: hal-01609221**

**<https://hal.science/hal-01609221>**

Submitted on 4 May 2018

**HAL** is a multi-disciplinary open access archive for the deposit and dissemination of scientific research documents, whether they are published or not. The documents may come from teaching and research institutions in France or abroad, or from public or private research centers.

L'archive ouverte pluridisciplinaire **HAL**, est destinée au dépôt et à la diffusion de documents scientifiques de niveau recherche, publiés ou non, émanant des établissements d'enseignement et de recherche français ou étrangers, des laboratoires publics ou privés.

# Reactivity enhancement of gasification biochars for catalytic applications

Marion Ducouso <sup>a,\*</sup>, Elsa Weiss-Hortala <sup>a</sup>, Ange Nzihou <sup>a</sup>, Marco J. Castaldi <sup>b</sup>

<sup>a</sup> Université de Toulouse, Mines Albi, CNRS, Centre RAPSODEE, Albi, France

<sup>b</sup> Chemical Engineering Department, City College, City University of New York, New York City, USA

## H I G H L I G H T S

- O<sub>2</sub> gas-phase treatment on biochars has been efficient.
- O<sub>2</sub> gas-phase treatment on biochars has been selective toward weak acids.
- The higher the temperature, the higher the oxygenation of the biochars surface.
- Specific surface area and porosity were significantly enhanced at 340 and 400 °C.

## Keywords:

Biochar  
Gasification  
Catalyst  
Oxygenated functions  
Reactivity  
Selectivity

## A B S T R A C T

To enhance the catalytic properties of woody biochars, an O<sub>2</sub> gas-phase treatment was performed at different temperatures (280, 340 and 400 °C) and times (2 h, 4 h, 8 h, 16 h) post-gasification. In fact the development of o-containing carbons based materials to increase their reactivity is gaining momentum. The efficacy and selectivity of the oxygen chemisorption on the biochars surface were investigated. FTIR revealed that the oxygenation has been efficient. Temperature Programmed Desorption (TPD) confirmed FTIR results and led to go further by providing quantitative results and insights into the selectivity. In fact the oxygen content at the surface was increased 1.3, 1.7 and 2.1 times after 2 h at 280, 340 and 400 °C respectively. At 280 °C, above 4 h of treatment the surface became saturated and the oxygen content was increased by 40%. The formation of weak acid functional groups has been enhanced without removing the basic functional groups already present on the surface. Carboxylic acids (strongest acids) were removed since they were not stable at the treatment temperature. The higher the total amount of o-containing functions, the more acid the pH<sub>pzc</sub>. The pH<sub>pzc</sub> of the raw biochars is of 3.1. At 280 °C even if the oxygenation was efficient it did not impact the global surface acidity. At highest temperature the higher amount of oxygenated functions decreased the pH<sub>pzc</sub> to reach and go below 2. Thus the chemisorption was efficient and selective. BET analyses showed that at highest temperatures (340 and 400 °C) the treatment increased the surface area and porosity. At 400 °C the specific surface area gained 15% and the porosity was increased 1.5 times whereas at 280 °C the specific surface area decreased to reach 80% of the initial surface area. These results highlight that the combustion has been enhanced at 340 and 400 °C which burnt carbon atoms and free the pores. Thus oxygenation at 340 or 400 °C is more interesting than at 280 °C since results have shown that the higher efficiency, specific surface area and porosity have been obtained under those conditions.

## 1. Introduction

Carbon materials have interesting surface properties to be used as adsorbents [1,2] catalysts [3] or catalytic supports [4,5]. Among the physico-chemical properties, surface oxygenated functional

groups have been recognized to influence performance. The development of O-containing carbon based materials is of great interest and is currently utilized in many catalytic applications such as electrode materials in supercapacitors [6], reduction of tetracycline and aromatic nitro compounds [7,8] SO<sub>2</sub> and NO<sub>x</sub> removal from flue gases [9] and dehydrogenation/dehydration of aliphatic alcohols. For example, Szymanski et al. concluded that acidic organic functions were active sites for hydrocarbon dehydrogenation and dehydration [10–13]. In addition, Teng et al. [9] have correlated the increase of the carbon material activity toward the reduction

\* Corresponding author at: RAPSODEE (office 0E012), Ecole des Mines d'Albi-Carmaux, Campus Jarlard, 81 013 Albi, France. Tel.: +33 5 63 49 32 40.

E-mail addresses: [marion.ducouso@mines-albi.fr](mailto:marion.ducouso@mines-albi.fr) (M. Ducouso), [elsa.weiss@mines-albi.fr](mailto:elsa.weiss@mines-albi.fr) (E. Weiss-Hortala), [ange.nzihou@mines-albi.fr](mailto:ange.nzihou@mines-albi.fr) (A. Nzihou), [mcastaldi@che.cuny.cuny.edu](mailto:mcastaldi@che.cuny.cuny.edu) (M.J. Castaldi).

**Table 1**  
Properties of the raw biochar (proximate and ultimate analyses).

Proximate analysis	
Moisture content (wt%)	6.2
Ash content (wt%)	3.6
Ultimate analysis	
Element (wt%)	
C	77.4
H	2.0
N	0.5
S	0
O (by difference)	16.5

\* (%O = 100 - %C - %H - %N - %S - %ash).

of NO with NH<sub>3</sub> to the enhancement of acidic functions, specifically the hydroxyl type groups. Therefore functionalization of solid surfaces with O-containing groups is of great interest to increase their reactivity.

Most of the studies about functionalization have been already performed on activated carbons from polymers sources, carbon black or coal chars which all come from fossil fuel feedstocks [14,15]. An emergent inexpensive candidate is biochar from biomass gasification. Typically considered as a residue, their physico-chemical properties can have application in the catalytic field [16,17]. Biochars are microporous material with a high surface area containing heterogeneous atoms such as metal or oxygen atoms imbedded in the carbon matrix. Different O-containing groups such as carboxylic acids, lactones, carbonyls, ethers or phenols structure have been identified on chars from biomass conversion [18]. Functionalization of their surface by increasing the oxygen content is an opportunity to further develop them as an inexpensive catalyst from renewable sources. Various methods of oxygenation have been investigated either in gas and liquid phase: such as nitric acid, phosphoric acid, hydrogen peroxide, nitrous oxide and ozone [18–20]. Liquid phase treatments are strong oxidizing agents however they tend to decrease the porosity significantly and therefore the surface area. Alternatively gas-phase treatments are known to enhance the porosity and are competitive toward oxygen chemisorption compare to liquid treatment [21].

In this study biochars from gasification of poplar wood have been oxygenated by an O<sub>2</sub> gas-phase treatment at various temperatures ranging from 280 °C to 400 °C and for several duration times between 2 h and 16 h. The aim of the process was to chemisorb oxygen at the surface to increase the oxygen content. However, during the O<sub>2</sub> gas-phase treatment at the mid-range temperature, some oxygen atoms react with the carbon matrix instead of chemisorb which is traduced by a mass loss. Thus the oxygen chemisorption is in competition with the combustion reaction. At the appropriate operating conditions, the combination of these two reactions has a positive effect on the char surface properties. The chemisorption increases the oxygen content while the moderate combustion enhances the porosity and the specific surface area thus counteracting any surface area reduction associated with the chemisorption. Oxygenation of solid surfaces has already been studied using model structures such as activated carbon or black carbon. Therefore the goal of this study is to evaluate the efficacy and selectivity of the oxygen chemisorption on raw biochars. This material has already shown catalytic activity for hydrocarbon cracking or tar reforming. Its high surface area, the defects in the carbon matrix and the inherent heterogeneity (oxygenated functions and mineral content) should play a role in its reactivity. Increasing the oxygenated content is an opportunity to enhance its catalytic activity for the reactions presented in the first paragraph. Moreover the development of oxygenated biochars as catalyst is a competitive alternative to the commercial metal doped catalysts. In addition this study discusses the competition between

the oxygenation and the combustion reactions for the different operating conditions (time and temperature). Firstly the oxygenation efficacy will be observed by FTIR and then its selectivity will be described using Temperature Program Desorption. In a second step the global acidity of the biochars surface is investigated and correlated to the total oxygen amount of the surface by measuring their pH<sub>pzc</sub>. Finally, the evolution of the porosity and the specific surface area are investigated and linked to the mass loss to evaluate the competition between oxygen chemisorption and combustion. The final goal is to determine the best conditions to obtain the greatest level of oxygenated functions at the char surface without porosity loss in order to increase the catalytic reactivity of biochars.

## 2. Experimental

The experiments were carried out in three main steps: first poplar wood has been gasified under steam in a fluidized bed. Afterwards, the raw biochars where harvested and then oxygenated under a mixture of 8 v% O<sub>2</sub>/92 v% N<sub>2</sub> for different operating conditions and finally the oxygenated biochars surface have been characterized by Temperature Program Desorption, FTIR, pH<sub>pzc</sub> and BET analyzer.

### 2.1. Raw char generation by gasification of poplar wood

65 g of poplar wood chips (furnished by Lithaspen company) have been gasified into a fluidized bed (custom-made stainless steel) at 750 °C during 30 min into a 90 v% H<sub>2</sub>O/10 v% N<sub>2</sub> mixture (purity: 99.5%) atmosphere of 1.5 Nm<sup>3</sup>/h. Prior to gasification, the poplar wood has been ground into chips of about 4 mm × 4 mm × 1 mm. The gasifier was 60 cm height with an internal diameter of 6 cm. A quartz frit was positioned at approximately 12 cm from the bottom to hold the biomass. To ensure the biomass remains in the reactor a second frit was put at the top of the reactor. Ten K-type thermocouples (IEC- KX-1) have been installed 5 cm apart throughout the vertical direction to measure the temperature profile. A thermocouple positioned at center height of 30 cm was connected to a temperature controller (IEC- KX-1). The heating rate was 20 °C/min. Steam was produced from a vapor generator (liquid brooks mass flow controller flowomega) and nitrogen (ultra high purity) flow rate was controlled by a mass flow controller (Brooks 3851S). Post-testing, gasification chars have been crushed and sieved to obtain particle diameter between 100 and 500 μm. Table 1 shows the elemental composition, the ash and moisture content of the raw biochar harvested from the gasifier.

### 2.2. Oxygenation of the biochars surface by O<sub>2</sub>/N<sub>2</sub> gas-phase treatment

Approximately 100 mg of char (named raw\_char) have been oxygenated in flow through micro-reactor (ChemBet Pulsar-model 05090) under a mixture of 8 v% O<sub>2</sub>/92 v% N<sub>2</sub> (ultra high purity) and a flow rate of 45 ml/min for various time durations (2 h, 4 h, 8 h and 16 h) at 280 °C. The choice of oxygen concentration was to enable better resolution of the time dependence of oxygen interaction.

The produced chars utilized in this study are named as follows: ox2h\_280C, ox4h\_280C, ox8h\_280C and ox16h\_280C respectively. Oxygenation has also been carried out at 340 °C and 400 °C for 2 h to serve as comparisons. These chars are called: ox2h\_340C and ox2h\_400C (see Table 2).

Oxygenation has been performed in a quartz U-tube with an internal diameter of 4 mm placed into an electrical furnace (Chembet Pulsar instrument). The char bed of 75 mm length was

**Table 2**  
Designation of the biochars.

#	Description	Temp of oxygenation (°C)	Oxygenation time (h)	Name of the sample
1	raw char	–	–	raw_char
2	n°1 oxygenated	280	2	ox2h_280C
3	n°1 oxygenated	280	4	ox4h_280C
4	n°1 oxygenated	280	8	ox8h_280C
5	n°1 oxygenated	280	16	ox16h_280C
6	n°1 oxygenated	340	2	ox2h_340C
7	n°1 oxygenated	400	2	ox2h_400C

maintained by quartz wool at the extremities. The Chembet furnace was equipped with two grounded thermocouples (K-type) one for control and the other one inserted into one branch of the U-tube to monitor for over temperature conditions. The biochar bed was heated to the oxygenation temperature under pure nitrogen with a heating rate of 5 °C/min. Once the oxygenation temperature was reached, the pure nitrogen (3.7 ultra high purity) was replaced by the 8 v% O<sub>2</sub>/92 v% N<sub>2</sub> mixture after twenty minutes. The oxygenation process was carried out in two steps because CO<sub>2</sub> was produced all over the process but was not coming from the same origin. During the heating CO<sub>2</sub> was produced due to the desorption of carboxylic acids which were not stable at the oxygenation temperature. Then, during the oxygenation, combustion produces CO<sub>2</sub>. To be able to differentiate the CO<sub>2</sub> production origin, the heating was performed under pure nitrogen. Once the CO<sub>2</sub> production was almost equal to zero, the 8 v% O<sub>2</sub>/92 v% N<sub>2</sub> mixture was introduced. The effluent gas phase was analyzed online using a gas chromatograph (Agilent 3000A) with four different columns and TCD detectors which allow the detection of He, N<sub>2</sub>, O<sub>2</sub>, H<sub>2</sub>, CH<sub>4</sub>, CO and CO<sub>2</sub>. Production of CO<sub>2</sub> and CO was observed during the process which means combustion occurs during the oxygenation. The mass loss during the oxygenation process has been calculated from the following equation:

$$ML = \frac{(m_i - m_f)}{m_i} \quad (1)$$

where  $m_i$  is the initial mass of the biochar sample and  $m_f$  is the final mass after the process.

### 2.3. Biochars surface characterization

The surfaces of raw and oxygenated biochars have been characterized by Temperature Program Desorption (TPD), FTIR, measure of their  $pH_{pzc}$  and BET.

#### 2.3.1. Temperature Programmed Desorption (TPD)

The Temperature Programmed Desorption (TPD) provides information about the nature and quantity of the different oxygenated groups at the surface of a solid. TPD of 50 mg of raw and functionalized chars have been performed in the ChemBet Pulsar instrument under a 25 ml/min of helium from 25 °C to 1100 °C with a heating rate of 5 °C/min. The same set-up as for the oxygenation was used (see Section 2.2). Gas production was monitored by both the TCD detector from the ChemBet Instrument and by a 3000a gas chromatograph from Agilent with four different columns and TCD detectors which allow the detection of He, N<sub>2</sub>, O<sub>2</sub>, H<sub>2</sub>, CH<sub>4</sub>, CO and CO<sub>2</sub>. The total production of CO<sub>2</sub> and CO were calculated from the integration of the area under the curve of the chromatograms. The

TCD detector provides a continuous signal but the separation of the components is not possible while the micro gas chromatograph does the differentiation but it only allows a semi-continuous analysis. Results of the micro gas chromatograph have been used for a quantitative comparison of the CO<sub>2</sub> and CO production during the TPD analyses. The deconvolution of the TCD signal has been performed on the TPRWin software furnished with the ChemBet Pulsar instrument.

#### 2.3.2. FTIR

FTIR spectroscopy has been performed to observe the carbon-oxygen bondings at the biochars surface. Prior FTIR analyses samples have been finely ground in a mortar and mixed in KBr. Spectra have been obtained from a Nicolet Impact 400D spectrometer by adding 32 accumulations at a resolution of 8 cm<sup>-1</sup>.

#### 2.3.3. $pH_{pzc}$

The  $pH_{pzc}$  of the different biochars has been performed to evaluate the global acidity of the surface. The pH at the point of zero charge is the pH above which the total surface of the carbon particle is negatively charged [22]. Prior to analysis buffer solutions fixed at pH = 2, pH = 3.1, pH = 4, pH = 7 and pH = 10 have been prepared and biochars have been crushed to obtain powder. 5 mg of powder have been immersed into 5 mL of buffered solution. After stabilization, the value of the zeta potential has been determined using a Zetasizer Nano ZS Malvern instrument.

#### 2.3.4. BET

Textural properties such as specific surface area and micropore volume could be determined by adsorption of an inert gas. BET analyses have been done on an ASAP 2010 apparatus from Micromeritics. Adsorption of argon has been monitored at 77 K until a relative pressure of 1. Prior argon adsorption a degassing step of 30 h under high vacuum at 200 °C has been performed. Specific surface area has been determined by application of the BET model. Pore size and pore volume have been evaluated using the Horvath-Kawazoe model.

## 3. Results and discussion

The discussion is first focused on the time dependence of the oxygenation process and afterwards the temperature effect is studied. The efficacy, selectivity, global acidity and the evolution of the porosity/specific surface area over the oxygenation are the four main points addressed in this section.

### 3.1. Impact of the oxygenation time of the o-containing groups

At 280 °C the oxygenation process has been stopped at 2 h, 4 h, 8 h and 16 h to investigate the time dependence of the oxygen chemisorption. First, the efficacy and selectivity were evaluated by FTIR and TPD analyses. Once the total amount of oxygenated functions at the different biochars surfaces was determined it has been correlated to the global acidity of the surface by measurement of the  $pH_{pzc}$ . Finally the evolution of the specific surface area and porosity have been carried out and correlated to the mass loss values.

#### 3.1.1. Efficacy

The goal of oxygen chemisorption is to increase the total O-containing functions at the biochar surface. Its efficacy has been evaluated using two complementary techniques: FTIR and TPD. FTIR spectroscopy is sensitive to the different carbon-oxygen bondings. Fig. 1 shows the 800–2000 cm<sup>-1</sup> region of FTIR spectra for the raw and functionalized biochars. All the spectra show bands in the

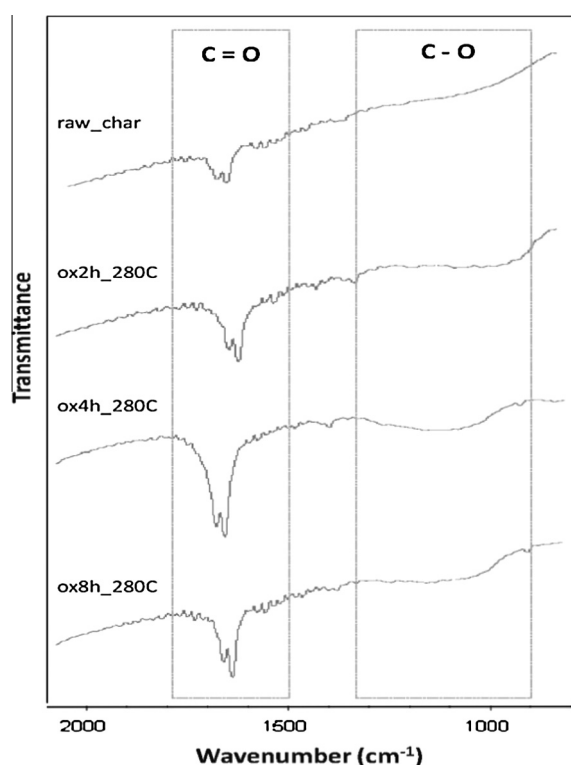


**Fig. 1.** Comparison of the 1000–2000  $\text{cm}^{-1}$  region of FTIR spectra of raw and oxygenated biochars at 280 °C.

region 1600–1800  $\text{cm}^{-1}$  corresponding to the C=O bonds associated with anhydrides, lactones, carboxylic and quinones (see Table 3). Profiles of the functionalized char at 280 °C for 2, 4 and 8 h display peaks similar to the raw char, but are more pronounced. A second large band is observable in Fig. 1 between 1000 and 1300  $\text{cm}^{-1}$  which corresponds to the C–O bonds of lactones, alcohol, phenol and ether (see Table 3). Thus FTIR spectra show that the different carbon–oxygen linkages have been increased after the  $\text{O}_2$  gas-phase treatment. However intensities of the different bands for the oxygenated chars are comparable and it is hard to conclude on the oxygenation time effect. Thus the TPD analysis has been used to provide more accurate understanding of the impact of the temperature and time of oxygenation on O-containing groups generated.

TPD is a dynamic analysis which consists of recording the production of  $\text{CO}_2$  and CO during the continual heating of the sample. Fig. 2 and Table 4 show the evolution and the total production of  $\text{CO}_2$  and CO over time for the raw and oxygenated chars at 280 °C (obtained from the micro gas chromatograph analyses).

**Table 3**  
FTIR peak assignments (adapted from [23]).

Related bands in Fig. 1	Wave number ( $\text{cm}^{-1}$ )	Functional group
C=O	1850–1786	Anhydrides
	1740,1724	Lactones (C=O)
	1710–1680	Carboxylic (C=O)
	1670–1660	Quinone or conjugated keton
C–O	1440	Carboxylic (O–H)
	1264	Lactones (C–O–C)
	1250–1235	Ether bridges between rings
	1162–1114	Phenol (C–O) and (O–H bend/stretching)
	1076–1014	Alcohol (C–O)

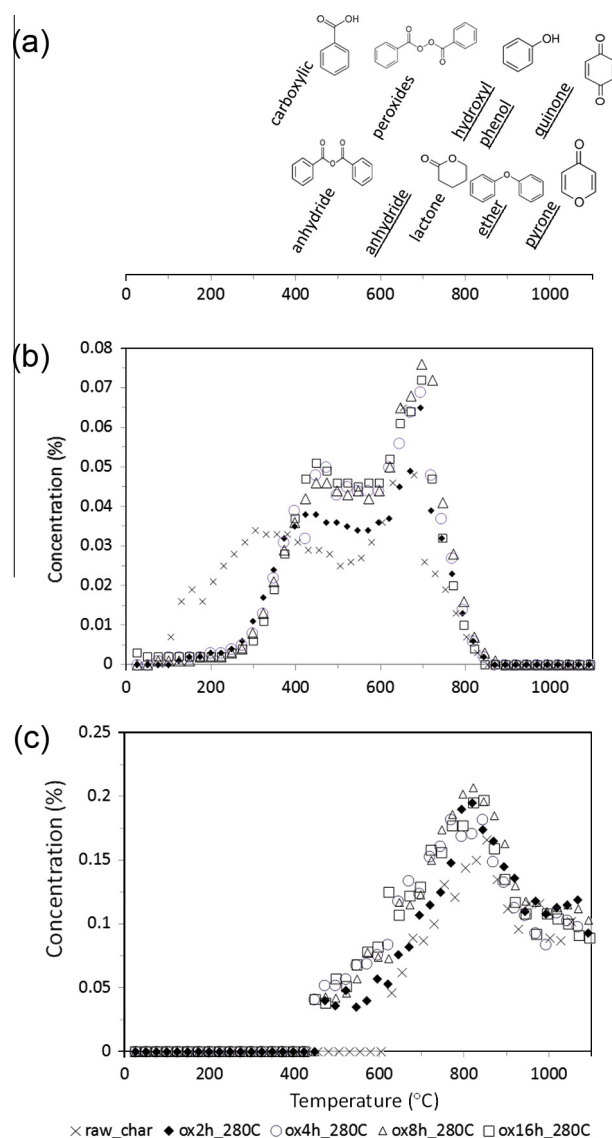


**Fig. 2.** An example of curve-fitting of the TPD curve with the TPRWin software from Quantachrome (char\_ox\_16h\_280 °C).

**Table 4**  
Comparison of  $\text{CO}_2$ , CO and total production for raw and functionalized chars oxygenated at 280 °C for different duration times (from the integration of the area under the curve of Fig. 2).

	$\text{CO}_2$	CO	Total	$\text{CO}_2/\text{CO}$
mmol/gchar				
raw_char	0.9	2.1	3.0	0.42
ox_2 h	0.8	3.0	3.9	0.28
ox_4 h	1.0	3.3	4.3	0.30
ox_8 h	1.0	3.5	4.5	0.29
ox_16 h	1.0	3.4	4.4	0.29

On Fig. 2 one can observe that both the production of  $\text{CO}_2$  and CO increased between 400 and 800 °C for the oxygenated chars. After 800 °C, the CO production is similar for all the samples and before 400 °C less  $\text{CO}_2$  is produced for the oxygenated chars which is explained by the loss of non-stable O-groups at that oxygenation temperature (this point is discussed more in detail in the selectivity part). The gases evolution over time is very interesting as well since we can observe that the curves of raw\_char and ox\_2 h

samples are well distinguished but the curves of ox\_4 h, ox\_8 h and ox\_16 h are superimposed meaning that a saturation is reached. Koch et al. [23] has done a similar study on coal char and observed a saturation of the surface after an increase of the oxygenated functions as well.

Results of the integration of the area under the curves of the Fig. 2 highlighted that the CO<sub>2</sub> and CO production were higher for the oxygenated chars than the raw chars (see Table 4). The total amount of oxygenated groups has been increased by a factor of 1.5 after 4 h of treatment since the raw\_char sample contained 3.0 mmol/g<sub>char</sub> and the ox4h\_280C sample 4.3 mmol/g<sub>char</sub>. Above 4 h of treatment the total amount of oxygenated functions remain almost stable. To conclude on the efficacy, the process has been successful and an increase of the total oxygenated functions was observable. However the total amount of O-groups must be regarded in terms of selectivity.

### 3.1.2. Selectivity

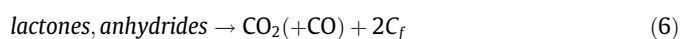
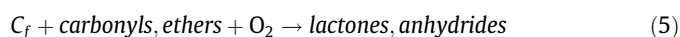
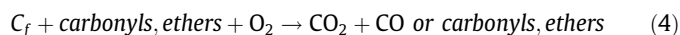
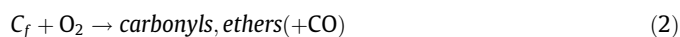
The next step is to evaluate the selectivity of the chemisorption with regard to the location of oxygen that was favored leading to the formation of some preferential groups. According to the literature, various types of oxygenated groups have been identified at the surface of the carbonaceous materials [24]. The theory of the TPD analyses is based on the distribution of desorption activation energies [25]. There is controversy in the literature over the assignment of the different peaks during TPD analyses. However some global trends have been established in previous studies [26–28]. CO<sub>2</sub> desorption is mainly due to acidic functions such as carboxylic and anhydride acids, it could also come from lactone or peroxide. Its production is observed in the 100–800 °C temperature range. Carboxylic acid desorption occurs at low temperature and lactone desorption at high temperature [27]. Carboxylic anhydrides produce both CO and CO<sub>2</sub> and a small difference in the desorption temperature is observed. Peroxides should produce a CO<sub>2</sub> peak at 550–600 °C [27]. CO which is produced above 600 °C could originate from the desorption of weak acids such as phenol or hydroxyl but also from neutral or basic functions such as pyrone-like structure, quinone, carbonyl and ethers functions [20,25,29]. Hydroxyl and phenols desorb and produce CO in the 600–800 °C temperature range and hydroxyl should desorb first. Pyrone-type structure and quinone (carbonyls) desorb at the highest temperature. In addition quinone desorb before pyrone-type structure. From the literature and the micro GC results, the signal has been deconvoluted using 13 Gaussians functions. The first one at 80 °C has been assigned to water evaporation. The CO<sub>2</sub> contribution was composed of 5 peaks: 1 for carboxylic acids at 390 °C, 1 for anhydrides at 450 °C, 1 for peroxides at 530 °C and 2 for lactones at 660 and 720 °C. Six peaks have been attributed to CO production: 1 for anhydrides at 590 °C, 1 for hydroxyl at 620 °C, 1 for phenol at 750 °C, 1 for ether at 844 °C, 1 for quinone at 880 °C and 1 for pyrone at 973 °C. In addition a negative peak at 870 °C for H<sub>2</sub> has been added. Peak temperatures (T<sub>m</sub>) were bound by ±50 °C and the Half Width at Half Maximum (HWHM) was kept constant. Fig. 3 presents an example of curve-fitting.

A first point of discussion is the evolution of the CO<sub>2</sub>/CO ratio over the process which is presented in Table 4. The initial CO<sub>2</sub>/CO ratio is of 0.42 for the raw biochar, after 2 h of treatment it decreases to 0.28. This difference is due to the loss of a part of the carboxylic acids (production of CO<sub>2</sub>) during the heating ramp under pure nitrogen prior the oxygenation at 280 °C. During the oxygenation both functions producing CO<sub>2</sub> and CO have been increased. Thus the ratio remains almost stable at 0.29 (±0.01).

Curves presented in Fig. 2 also show that the CO<sub>2</sub> production for the raw-char sample starts near 100 °C whereas it begins closer to 300 °C for functionalized chars. Thus carboxylic acids desorb during the heating ramp and were not formed during the

oxygenation as the temperature was too high, the concentration of carboxylic acids has been decreased by a factor of four after the oxygenation process. Conversely peroxides and lactones have been increased 2.1 and 1.2 times respectively (see Fig. 2b). The anhydride groups desorb in both CO<sub>2</sub> and CO at 450 °C and 580 °C respectively. Raw chars did not contain this type of function since the CO production started above 620 °C. However after oxygenation, Fig. 2 shows that the CO light-off temperature is lower for the functionalized samples compared to raw char indicating that anhydrides have been created.

On Fig. 2c it is observable that the shoulder near 700 °C increases suggesting that hydroxyl/phenolic groups are enhanced. Quinone and pyrone groups were apparently not impacted by the process. Results of the deconvolution show that hydroxyl, phenol and ether have been increased by a factor of 2.6, 1.7 and 1.3 respectively whereas quinones and pyrones concentrations have not been impacted. Therefore the oxygenation process seems to be selective. Figueiredo et al. [21] also concluded on oxygenation selectivity, especially CO-based functions, over commercial activated carbons (under a 5v% O<sub>2</sub>/N<sub>2</sub> mixture at 425 °C). With the extent of oxidation they also observed that the shoulder of the CO curve at low temperature became more predominant. They proposed an interpretation of this observation from the scheme described below proposed by Zhuang et al. [30]. This scheme presents the first possible interactions between oxygen, carbon atoms and oxygenated functions present at the surface. Secondary reactions or chain reactions such as Boudouard reaction or Water Gas shift reactions were not included in the following scheme:

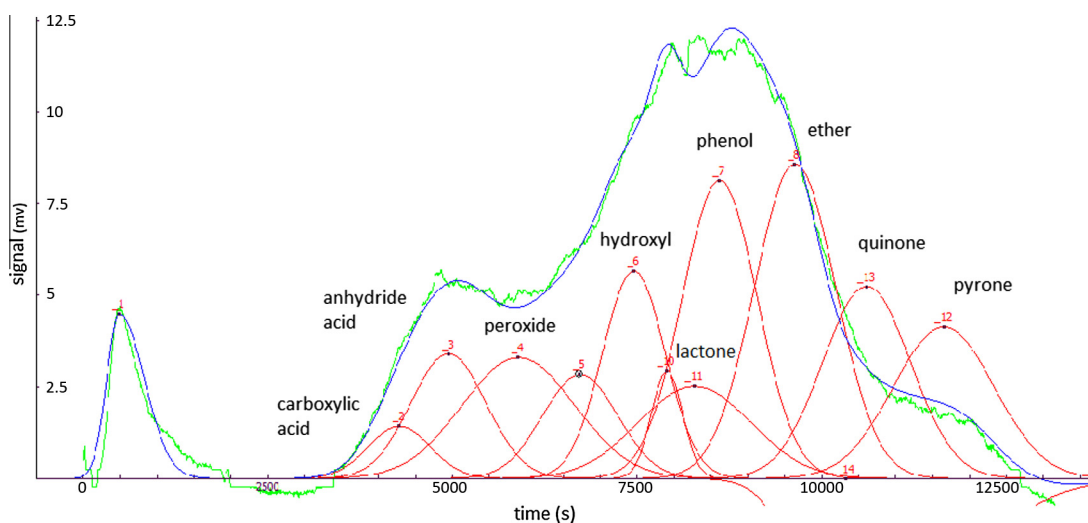


$C_f$  : carbon sites

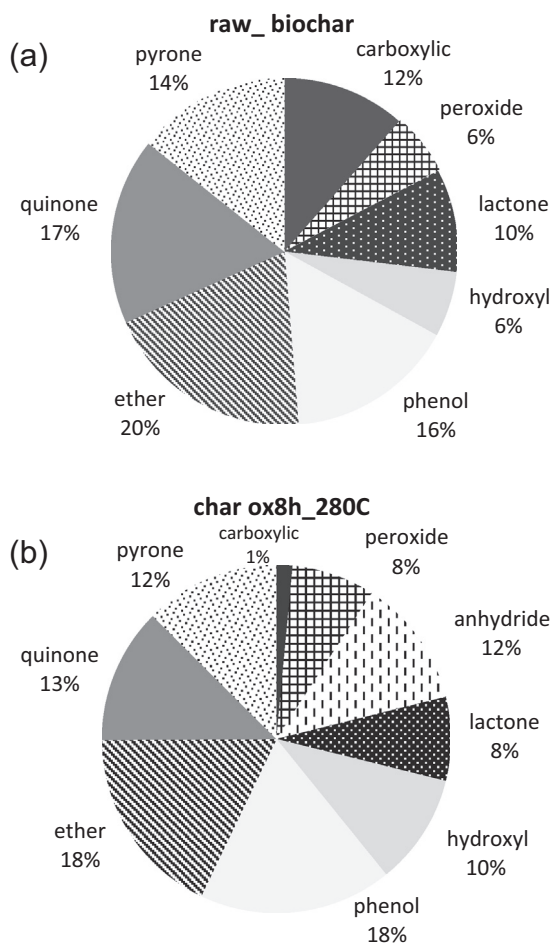
Phenol, ether, quinone and pyrone are the dominant functions on the raw biochar surface. Reactions (2) and (4) are not favored which explains that no increase of quinones and pyrone are observed. However reaction (5) where oxygen reacts with carbonyl and ethers already present at the surface to form lactones, anhydrides at higher extent seem to be the predominant reaction. Fanning et al. [31], also investigated oxidation of carbons under a mixture of O<sub>2</sub>/Ar. They stated that oxidation by O<sub>2</sub> gave evidence for initial formation of cyclic ethers. More complete oxidation produced cyclic anhydrides, lactones, phenols and ethers.

Fig. 4 shows that phenol, ether, quinone and pyrone are the main O-containing functions onto raw\_char surface with percentages of 16%, 20%, 17% and 14%. However after oxygenation only ether and phenol remain at 18% while quinone and pyrone contributions decreased to 12% because of the increase of hydroxyl, peroxides, lactones and the creation of anhydrides functions. Regarding anhydrides acids after 8 h of oxygenation they account for 12% of the total oxygenated functions whereas the raw biochars did not contain this type of function.

To conclude the oxygenation at 280 °C mainly leads to increase the amount of oxygenated functions such as peroxides, lactones, hydroxyl and phenol which could be gathered into two main groups: the functions containing a –OH groups (hydroxyl and



**Fig. 3.** Micro GC results during TPD of raw and functionalized chars oxygenated at 280 °C for different times: (a) scheme of the temperature desorption of the O-containing groups (in normal type face: groups producing CO<sub>2</sub>, underlined: groups producing CO); (b) CO<sub>2</sub> production; (c) CO production.



**Fig. 4.** Oxygenated groups distribution in atom% of raw chars (a) and chars oxygenated 8 h at 280C (b).

phenol) and those composed of one (or more) atoms inserted into a carbon ring or carbon chain (peroxide, lactone). Anhydrides functions have been created as well and take part of the second categories of functions. This trend is coherent since the raw char surface was mainly covered by edge carbon functions such as

**Table 5**

Specific surface area, total micropore volume and mass loss of the raw and functionalized chars at 280 °C for different oxygenation times (2 h, 4 h, 8 h).

Sample	$S_{BET}$ (m <sup>2</sup> /g)	$V_{micro}$ (cm <sup>3</sup> /g)	Mass-loss
raw_char	573.8	0.219	0
ox2h_280C	530.5	0.216	7.1
ox4h_280C	475.1	0.207	11.1
ox8h_280C	464.1	0.204	11.6

quinone and pyrone-like structures. Oxygenation at 280 °C favored the formation of weak acid functions without removing basic groups such as quinone or pyrone. However the process reduce the amount of carboxylics, which are the strongest acids, by a factor of four. Thus the global amount of the oxygenated functions has been increased 1.5 keeping the duality of acidic and basic characters even if the new acidic functions at the functionalized biochars surface are less strong than the one of the raw chars.

### 3.1.3. Global acidity

The acidity of the surface is related to the oxygenated content and was investigated by measuring their  $pH_{pzc}$ . The pH of the raw chars and the functionalized chars are 3.1 and between 2 and 4 respectively. Literature reports the investigation of a correlation between the content of O-containing groups and the  $pH_{pzc}$  [32–34]. A relationship has been established [22] and it shows that the  $pH_{pzc}$  decreases rapidly as the oxygen content increases from 0 to 3 mmol/g. Typically a  $pH_{pzc}$  of about 9 corresponds to a low value of oxygenated groups (1 mmol/g). From 2 mmol/g of O-containing groups at the carbon surface the value of  $pH_{pzc}$  is under 4 and stabilizes between 3.5 and 2 for higher values of oxygen functions. Jaramillo et al. [35] studied different methods of oxygenation on activated carbons and observed the same trend. In this study the raw-char sample contains already 3.0 mmol/gchar and the content of the functionalized chars has been increased. The values of the  $pH_{pzc}$  are stable in the 2–4 range which is coherent with the relationship established in the literature.

### 3.1.4. BET specific surface area, porosity and mass loss

Oxygenation at moderate temperature leads to two competitive reactions: combustion of a part of the biochars carbon structure appears while oxygen atoms adsorbed at the surface. This is

confirmed by the mass loss which increases up to 4 h of treatment (see Table 5) and the production of CO<sub>2</sub> and CO during the oxygenation process. These two reactions should have an opposite effect on the porosity. Combustion which burns carbon atoms from the surface should enhance the porosity by freeing the pores whereas chemisorption which leads to addition of oxygen atoms tends to fill the pores and decrease the specific surface area. BET analyses of the different biochars have been performed to statue which reaction has the predominant effect on the surface area and total microporosity. Table 5 provides BET surface area and micropore volume of the raw and functionalized chars. The raw char is a microporous material with a specific surface area of 573.8 m<sup>2</sup>/g and a micropore volume of 0.219 cm<sup>3</sup>/g. At 280 °C all functionalized chars exhibit both smaller surface area and micropore volume than the raw\_char sample. The specific surface area has been decreased by 20% after 4 h of treatment. Then chemisorption has been the predominant phenomenon and pores tend to have been filled. As the total oxygen amount and the surface area were determined for the different biochars, an estimation of the surface occupied by oxygen atoms at the biochars surface has been investigated. For the calculation, a value of 0.083 nm<sup>2</sup> was assigned as the average area occupied by one oxygen atom chemisorbed on one carbon site on the primastic places of the surface [36,37]. The surface occupied by oxygen atoms at the raw\_char surface has been evaluated to 159.2 m<sup>2</sup>/g which represents 27% of the BET surface area of the raw char. At saturation after 8 h of treatment the percentage of surface covered by oxygen is estimated at 51%.

### 3.1.5. Partial conclusion on the impact of the oxygenation times

The oxygenation time played an important role since the longer the oxygenation, the higher the oxygen amount was chemisorbed until the saturation was reached. Oxygenation at 280 °C above 4 h of oxygenation provides biochars containing 1.5 more oxygenated functions at their surface with both an acidic and basic character since the process increased weak acids such as anhydrides, peroxides and hydroxyl functions and did not remove basic groups. It has been observed that carboxylic amount was diminished by 4 after the treatment. Even if they are the strongest acids the global acidity of the surface remained unchanged since their loss was made up by the addition of the weak acids. Combustion during the O<sub>2</sub> gas-phase treatment has been detected by the increase of the mass loss but it was not severe enough to counterbalance the oxygen chemisorption at the biochars surface. In fact the specific surface area has been decreased by 20%. Thus we obtained good insights into evolution of the oxygenated functions arrangement over the process of oxygenation. Regarding the surface properties of the functionalized biochar the oxygenation at 280 °C has been successful. The global amount of the oxygenated functions has been increased by 50% but the specific surface area was diminished by 20%.

## 3.2. Impact of the oxygenation temperature on the O-containing groups

The temperature dependence of the oxygen chemisorption is the topic of this section. Temperature should increase the oxygen chemisorption thus higher oxygen content should adsorb at the surface. However combustion is sensitive to the temperature as well and could become the dominant reaction. Thus efficacy and selectivity of oxygen chemisorption on biochar surface is evaluated and discussed, especially as regards to the combustion reaction. The same approach as in 3.1 was developed to study the impact of the temperature on the oxygenated content, global acidity, porosity and mass loss of the chars.

### 3.2.1. Efficacy

FTIR applied to samples obtained after oxygenation at three temperatures demonstrated that the intensity of the bands corresponding to oxygenated functions increased (not shown). Therefore oxygenation was also successfully achieved. The amounts of CO and CO<sub>2</sub> desorbed during TPD are presented in Table 6 (obtained from the integration of the area under the curve of Fig. 5). The total amount of CO and CO<sub>2</sub> is 1.9 and 2.1 times higher after the oxygenation at 340 and 400 °C respectively. Temperature had a more significant impact on the oxygen chemisorption than the oxygenation times since the total amount was doubled in 2 h at 400 °C and as recorded it was increased 1.5 times after 4 h at 280 °C. Although combustion reaction occurred at the same time TPD and FTIR results highlight that the oxygenated functions amount has been increased. The CO<sub>2</sub>/CO is also varying as the oxygenation temperature increases meaning that O-functions are selectively increased.

### 3.2.2. Selectivity and gobal acidity

Fig. 5 shows a comparison of the CO<sub>2</sub> and CO production of TPD analyses recorded by micro-GC when oxygenation temperature increases. CO<sub>2</sub> and CO profiles at 340 and 400 °C are significantly higher than those of the raw\_char and functionalized biochar at 280 °C.

As shown in Fig. 5, the CO<sub>2</sub> production profile of the samples ox2h\_340C and ox2h\_400C are different from the raw\_char. One large peak between 400 and 800 °C is observable meaning that groups desorbing in this temperature range (anhydride, peroxide, lactone, hydroxyl and phenol) should have been significantly increased. In fact peroxides were enhanced 3.1 and 4.6 times at 340 °C and 400 °C respectively. Regarding the lactone group, their amount has been enhanced by a factor of 1.6 and 2.0 at 340 and 400 °C. Anhydrides have also been formed at these temperatures. They represent 11% and 10% of the total oxygenated functions for the samples ox2h\_340C and ox2h\_400 °C (see Fig. 6). Fig. 5.c highlights that hydroxyl and phenol have been significantly increased while ether, quinone and pyrone amounts remain stable. Results of the deconvolution show that hydroxyl amount was raised by a factor of 4 and 7 after oxidation at 340 and 400 °C respectively. The amount of phenol was nearly twice higher than the amount on the raw biochars after the two oxygenation processes. On the other hand carboxylic acids have been completely desorbed at these temperatures of oxygenation. Fig. 6 shows the distribution of the O-containing groups at the surface of sample ox2h\_340C and ox2h\_400C. Predominant functions are phenol and hydroxyl with percentages of 24%, 20% and 17%, 21% respectively. Quinone and pyrone groups became the smaller percentages of the O-containing groups (9%). Oxygenation at 340 °C and 400 °C promotes the enhancement of weak acidic functions at the char surface without removing the basics groups. At 400 °C, the CO<sub>2</sub>/CO ratio reaches 0.37 since the significant formation of peroxides, anhydrides and lactones balance the loss of carboxylic groups. Although the oxygenation increases slightly weak acidic functions, the pH<sub>pzc</sub> of the char oxygenated at 340 and 400 °C are of 2 and below 2 respectively. These results are coherent with the literature

**Table 6**  
Comparison of CO<sub>2</sub>, CO and total production of raw\_chars, ox2h\_280C, ox2h\_340C, ox2h\_400C obtained (from the integration of the area under the curve of Fig. 5).

	tot CO <sub>2</sub>	tot CO	tot	CO <sub>2</sub> /CO
	mmol/g <sub>char</sub>			-
raw_char	0.9	2.1	3.0	0.42
ox2h_280C	0.8	3.0	3.8	0.26
ox2h_340C	1.2	4.0	5.2	0.29
ox2h_400C	1.7	4.6	6.3	0.37



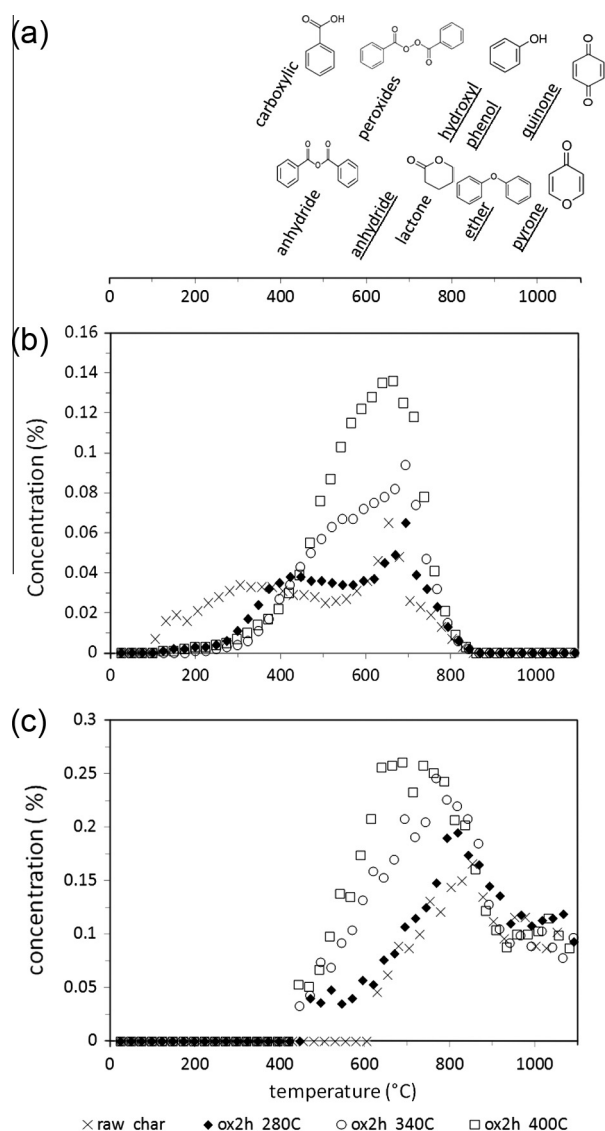


**Fig. 5.** Micro GC results during TPD of raw and functionalized chars oxygenated at 280 °C, 340 °C and 400 °C for 2 h: (a) scheme of the temperature desorption of the O-containing groups (in normal type face: groups producing CO<sub>2</sub>, underlined: groups producing CO); (b) CO<sub>2</sub> production; (c) CO production.

and the discussion in the Section 3.1. The oxygen content of these two chars is higher compared to the one of the raw chars which has a  $pH_{pzc}$  of 3.1. The high amount of oxygen function decreased the  $pH_{pzc}$  of these chars.

### 3.2.3. BET specific surface area, porosity and mass loss

Table 7 shows the specific surface area, porosity and mass loss of the raw and functionalized chars. At 340 and 400 °C, the oxygenation increased significantly the porosity and specific surface area. At 400 °C, the porosity is enhanced by 1.5 while the specific surface area gained 15%. The mass loss reaches 26.5% which is about 4 times higher than the one of the biochars oxygenated at 280 °C for 2 h. Thus combustion has been enhanced at higher temperature. Some oxygen atoms should have reacted with carbon atoms from the biochars surface. In fact CO<sub>2</sub> and CO productions have been enhanced during the oxygenations at 340 and 400 °C. Those operating conditions free the pores instead of filling them (oxygenation at 280 °C). The oxygenated biochars remain microporous.

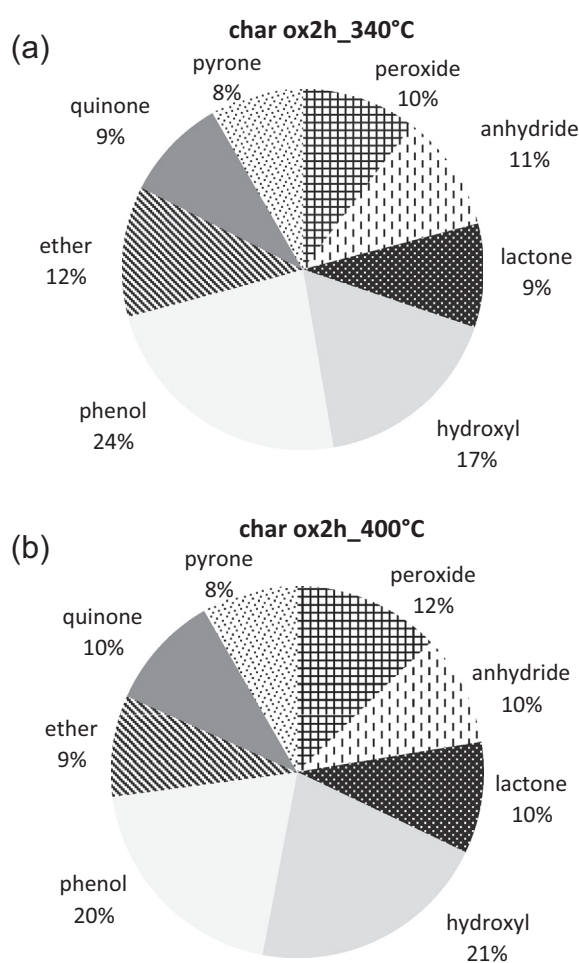


**Fig. 6.** Oxygenated groups distribution in atom% of ox2h\_340C (a) and ox2h\_400C (b).

**Table 7**

Specific surface area, porosity and mass loss of the raw and functionalized chars oxygenated at 280, 340 and 400 °C for 2 h.

Sample	$S_{BET}$ (m <sup>2</sup> /g)	$V_{micro}$ (cm <sup>3</sup> /g)	Mass loss (%)
raw_char	573.8	0.219	0
ox2h_280C	530.5	0.216	7.1
ox2h_340C	627.1	0.301	12.2
ox2h_400C	666.8	0.323	26.5

### 3.2.4. Partial conclusion on the impact of the oxygenation temperature

The oxygenation at 340 and 400 °C were more efficient rather than at 280 °C since the total oxygen amount adsorbed on the biochar was increased 1.9 and 2.1 times respectively whereas it was increased 1.3 times after 2 h at 280 °C. Thus the oxygenation temperature plays a decisive role regarding the efficacy of the oxygenation. Hydroxyl, phenol, peroxides and lactones were the preferential functions enhanced, especially hydroxyl. The oxygen treatment was beneficial for the specific surface area and porosity. At 400 °C, the porosity has been enhanced by 1.5 while the specific surface area gained 15%. Literature highlights that carbon catalyst containing both acidic and basic O-containing groups are very interesting and competitive compared to commercial catalyst for the destruction of methyl tertiary butyl ether [11] or the SO<sub>x</sub> and NO<sub>x</sub> abatement [9]. In fact this kind of catalytic reactions are usually performed in a low temperature range (between 80 and

200 °C) which is adapted for the utilization of the oxygenated biochars as catalyst since all the added oxygenated functions during the oxygenation process are stable up to 200 °C.

#### 4. Conclusion

The oxygenation has been used to enhance the reactivity of gasification biochars. It has been shown that the oxygenation was successful over times (2–16 h) and operating temperatures (280–400 °C). However the higher the temperature was, the more efficient the oxygenation was. Whatever the conditions, the process is selective toward weak acids formation and the selectivity is enhanced at higher temperature. In addition, the combustion has a beneficial impact on porosity at high oxygenation temperature because it frees the pores. Indeed, at 400 °C the process leads to increase twice the total amount of oxygen atoms at the surface compared to raw biochar, while the increase is only of 1.3 at 280 °C. Oxygenation leads to an increase of selective O-groups. Especially, formations of weak acid functions containing a —OH groups (hydroxyl and phenol) and those composed of one (or more) atoms inserted into a carbon ring or carbon chains (lactone, anhydrides, peroxides) were favored since the raw biochars surface was mainly composed of C=O functions (carbonyl, pyrone). Hydroxyl groups were particularly favored as the oxygenation temperature increased. After oxygenation biochars contain both acidic and basic functions. Porosity and specific surface area were enhanced significantly for the oxygenation reaction at 340 and 400 °C. At 400 °C, the porosity has been enhanced by 1.5 while the specific surface area gained 15%. Overall the results presented support the relevance of the oxygenation to increase the oxygenated groups at the surface of the biochars. This should lead to the increase of the reactivity for catalytic reactions presented in the introduction paragraph. Hence these catalytic reactions are performed at quite low temperature (below 200 °C). Added oxygenated functions at the biochars surface will be stable in this range of temperature.

#### Acknowledgments

This research was supported by the RAPSODEE Center at the Ecole des Mines d'Albi-Carmaux and the Earth Engineering Center at the City College of New York. The authors thank Sylvie Delconfetto, Séverine Patry and Jean-Marie Sabathier for assistance with experiments.

#### References

- [1] Liu W-J, Zeng F-X, Jiang H, Zhang X-S. Preparation of high adsorption capacity bio-chars from waste biomass. *Bioresour Technol* 2011;102:8247–52. <http://dx.doi.org/10.1016/j.biortech.2011.06.014>.
- [2] Mohan D, Rajput S, Singh VK, Steele PH, Pittman CU. Modeling and evaluation of chromium remediation from water using low cost bio-char, a green adsorbent. *J Hazard Mater* 2011;188:319–33. <http://dx.doi.org/10.1016/j.jhazmat.2011.01.127>.
- [3] Rodriguez-Reinoso F. The role of carbon materials in heterogeneous catalysis. *Carbon N Y* 1998;36:159–75.
- [4] Sobana N, Swaminathan M. Combination effect of ZnO and activated carbon for solar assisted photocatalytic degradation of Direct Blue 53. *Sol Energy Mater Sol Cells* 2007;91:727–34. <http://dx.doi.org/10.1016/j.solmat.2006.12.013>.
- [5] Barroso-Bogeat A, Alexandre-Franco M, Fernández-González C, Gómez-Serrano V. Preparation of activated carbon–metal oxide hybrid catalysts: textural characterization. *Fuel Process Technol* 2014;126:95–103. <http://dx.doi.org/10.1016/j.fuproc.2014.04.022>.
- [6] Sereydych M, Hulicova-Jurcakova D, Lu GQ, Bandosz TJ. Surface functional groups of carbons and the effects of their chemical character, density and accessibility to ions on electrochemical performance. *Carbon N Y* 2008;46:1475–88. <http://dx.doi.org/10.1016/j.carbon.2008.06.027>.
- [7] Liu P, Liu W-J, Jiang H, Chen J-J, Li W-W, Yu H-Q. Modification of bio-char derived from fast pyrolysis of biomass and its application in removal of tetracycline from aqueous solution. *Bioresour Technol* 2012;121:235–40. <http://dx.doi.org/10.1016/j.biortech.2012.06.085>.
- [8] Fujita S, Watanabe H, Katagiri A, Yoshida H, Arai M. Nitrogen and oxygen-doped metal-free carbon catalysts for chemoselective transfer hydrogenation of nitrobenzene, styrene, and 3-nitrostyrene with hydrazine. *J Mol Catal A Chem* 2014;393:257–62. <http://dx.doi.org/10.1016/j.molcata.2014.06.021>.
- [9] Teng H, Tu Y, Lai Y, Lin C. Reduction of NO with NH<sub>3</sub> over carbon catalysts The effects of treating carbon with H<sub>2</sub>SO<sub>4</sub> and HNO<sub>3</sub>. *Carbon N Y* 2001;39:575–82.
- [10] Szymanski GS, Rychlicki G, Terzyk AP. Catalytic conversion of ethanol on carbon catalysts. *Carbon N Y* 1994;32:265–71.
- [11] Szymański GS. Catalytic destruction of methyl tertiary butyl ether (MTBE) using oxidized carbon. *Catal Today* 2008;137:460–5. <http://dx.doi.org/10.1016/j.cattod.2008.01.003>.
- [12] Szymanski GS, Rychlicki G. Catalytic conversion of propan-2-ol on carbon catalysts. *Carbon N Y* 1993;31:247–57.
- [13] Szymański GS, Rychlicki G. Importance of oxygen surface groups in catalytic dehydration and dehydrogenation of butan-2-ol promoted by carbon catalysts. *Carbon N Y* 1991;29:489–98. [http://dx.doi.org/10.1016/0008-6223\(91\)90112-V](http://dx.doi.org/10.1016/0008-6223(91)90112-V).
- [14] Pastrana-Martínez LM, Morales-Torres S, Likodimos V, Falaras P, Figueiredo JL, Faria JL, et al. Role of oxygen functionalities on the synthesis of photocatalytically active graphene–TiO<sub>2</sub> composites. *Appl Catal B Environ* 2014;158–159:329–40. <http://dx.doi.org/10.1016/j.apcatb.2014.04.024>.
- [15] Perrard A, Retailliau L, Berjoan R, Joly J-P. Liquid phase oxidation kinetics of an ex-cellulose activated carbon cloth by NaOCl. *Carbon N Y* 2012;50:2226–34. <http://dx.doi.org/10.1016/j.carbon.2012.01.039>.
- [16] Klinghoffer NB, Castaldi MJ, Nzihou A. Catalyst properties and catalytic performance of char from biomass gasification. *Ind Eng Chem Res* 2012. <http://dx.doi.org/10.1021/ie3014082>.
- [17] Klinghoffer NB, Castaldi MJ, Nzihou A. Influence of char composition and inorganics on catalytic activity of char from biomass gasification. *Fuel* 2015. <http://dx.doi.org/10.1021/ie3014082>.
- [18] El-Hendawy A-NA. Variation in the FTIR spectra of a biomass under impregnation carbonization and oxidation conditions. *J Anal Appl Pyrolysis* 2006;75:159–66. <http://dx.doi.org/10.1016/j.jaap.2005.05.004>.
- [19] Xianglan Z, Shengfu D, Qiong L, Yan Z, Lei C. Surface functional groups and redox property of modified activated carbons. *Min Sci Technol* 2011;21:181–4. <http://dx.doi.org/10.1016/j.mstc.2011.02.020>.
- [20] Otake Y, Jenkins RG. Characterization of oxygen-containing surface complexes created on a microporous carbon by air and nitric acid treatment. *Carbon N Y* 1993;31:109–21.
- [21] Figueiredo JL, Pereira MFR, Freitas MMA, Orfao JJM. Modification of the surface chemistry of activated carbons. *Carbon N Y* 1999;37:1379–89.
- [22] Lopez-Ramon MV, Stoeckli F, Moreno-Castilla C, Carrasco-Marín F. On the characterization of acidic and basic surface sites on carbons by various techniques. *Carbon N Y* 2000;37:1215–21.
- [23] Kochan A, Krzton A, Fiqueneisel G. A study of carbonaceous char oxidation in air by semi-quantitative FTIR spectroscopy. *Fuel* 1998;77:563–9.
- [24] Figueiredo JL, Pereira MFR. The role of surface chemistry in catalysis with carbons. *Catal Today* 2010;150:2–7. <http://dx.doi.org/10.1016/j.cattod.2009.04.010>.
- [25] Zhang L-H, Calo J. Thermal desorption methods for porosity characterization of carbons and chars. *Colloids Surf A Physicochem Eng Asp* 2001;187–188:207–18. [http://dx.doi.org/10.1016/S0927-7757\(01\)00633-1](http://dx.doi.org/10.1016/S0927-7757(01)00633-1).
- [26] Karpinski Z, Szymanski GS. The effect of the gradual thermal decomposition of surface oxygen species on the chemical and catalytic properties of oxidized activated carbon. *Carbon N Y* 2002;40:2627–39.
- [27] Zhou J-H, Sui Z-J, Zhu J, Li P, Chen D, Dai Y-C, et al. Characterization of surface oxygen complexes on carbon nanofibers by TPD, XPS and FT-IR. *Carbon N Y* 2007;45:785–96. <http://dx.doi.org/10.1016/j.carbon.2006.11.019>.
- [28] Zielke U, Huttering K, Hoffman W. Surface-oxidized carbon fibers: I. surface structure and chemistry. *Carbon N Y* 1996;34:983–98.
- [29] Salame II, Bandosz TJ. Surface chemistry of activated carbons: combining the results of temperature-programmed desorption, boehm, and potentiometric titrations. *J Colloid Interf Sci* 2001;240:252–8. <http://dx.doi.org/10.1006/jcis.2001.7596>.
- [30] Zhuang Q, Kyotani T, Tomita A. DYNAMICS OF SURFACE OXYGEN COMPLEXES DURING CARBON GASIFICATION WITH OXYGEN. *Energy Fuels* 1995;9:630–4.
- [31] Fanning PE, Vannice MA. A drift study of the formation of surface groups on carbon by oxidation. *Carbon N Y* 1991;31:721–30.
- [32] Menendez JA. On the distribution of oxygen-containing surface groups in carbons and their influence on the preparation of carbon-supported molybdenum catalysts. *Solid State Ionics* 1998;112:103–11.
- [33] Borah D, Satokawa S, Kato S, Kojima T. Surface-modified carbon black for As(V) removal. *J Colloid Interf Sci* 2008;319:53–62. <http://dx.doi.org/10.1016/j.jcis.2007.11.019>.
- [34] Arenillas A, Pevida C, Rubiera F, Palacios JM, Navarrete R, Denoyel R, et al. Surface characterisation of synthetic coal chars made from model compounds. *Carbon N Y* 2004;42:1345–50. <http://dx.doi.org/10.1016/j.carbon.2004.01.017>.
- [35] Jaramillo J, Alvarez PM, Gómez-Serrano V. Oxidation of activated carbon by dry and wet methods. *Fuel Process Technol* 2010;91:1768–75. <http://dx.doi.org/10.1016/j.fuproc.2010.07.018>.
- [36] Ismail IM, Walker P. Rates and heats of oxygen chemisorption on Saran chars at 100 °C. *J Colloid Interf Sci* 1980;75:299–312. [http://dx.doi.org/10.1016/0021-9797\(80\)90454-3](http://dx.doi.org/10.1016/0021-9797(80)90454-3).
- [37] Vautard F, Dentzer J, Nardin M, Schultz J, Defoort B. Influence of surface defects on the tensile strength of carbon fibers. *Appl Surf Sci* 2014;322:185–93. <http://dx.doi.org/10.1016/j.apsusc.2014.10.066>.